Reviews

Particle Manipulation with External Field; From Recent Advancement to Perspectives

Akihisa Miyagawa*† and Tetsuo Okada†**

*Department of Chemistry, Faculty of Pure and Applied Science, University of Tsukuba, Tsukuba, Ibaraki 305–8577, Japan
**Department of Chemistry, Tokyo Institute of Technology, Meguro, Tokyo 152–8551, Japan

Physical forces, such as dielectric, magnetic, electric, optical, and acoustic force, provide useful principles for the manipulation of particles, which are impossible or difficult with other approaches. Microparticles, including polymer particles, liquid droplets, and biological cells, can be trapped at a particular position and are also transported to arbitrary locations in an appropriate external physical field. Since the force can be externally controlled by the field strength, we can evaluate physicochemical properties of particles from the shift of the particle location. Most of the manipulation studies are conducted for particles of sub-micrometer or larger dimensions, because the force exerted on nanomaterials or molecules is so weak that their direct manipulation is generally difficult. However, the behavior, interactions, and reactions of such small substances can be indirectly evaluated by observing microparticles, on which the targets are tethered, in a physical field. We review the recent advancements in the manipulation of particles using a physical force and discuss its potentials, advantages, and limitations from fundamental and practical perspectives.

Keywords Particle manipulation, external field, physical force, particle trapping

(Received August 17, 2020; Accepted September 7, 2020; Advance Publication Released Online by J-STAGE September 11, 2020)

1 Introduction

Micro/nanoparticles are widely employed for various purposes not only in scientific studies but also in industrial practices.[1–7] In particular, bioparticles, including multicellular organisms, cells, bacteria, viruses, and extracellular particles have received extensive attention, and there is strong methods for the demand for effective separation and manipulation of bioparticle.[8,9] The principles for particle separation are classified into passive and

Aihisa Miyagawa is an Assistant Professor of the Department of Chemistry, Pure and Applied Science, University of Tsukuba. He received his M.S. and Ph.D degrees from Tokyo Institute of Technology. His research interests are acoustofluidics, surface chemistry, and trace analysis. He is studying the development of novel trace detection schemes based on micro/nanoparticle behavior in various external fields, such as acoustic, electric, and optical field.

Tetsuo Okada received his B.S., M.S., and Ph.D. degrees from Kyoto University. He was appointed to Assistant Professor at Shizuoka University in 1986 and Associate Professor in 1989. He joined Tokyo Tech in 1995 and was promoted to Full Professor in 2000. His research interests are in various facets of separation science, interfacial phenomena, and solution chemistry. His laboratory members are mostly studying the chemistry of ice and frozen solutions, phenomena occurring at the ice/solution interface, and the functions of ice in natural environments and biological systems.

† To whom correspondence should be addressed.
E-mail: miyagawa.akihisa.gf@u.tsukuba.ac.jp (A. M.); tokada@chem.titech.ac.jp (T. O.)

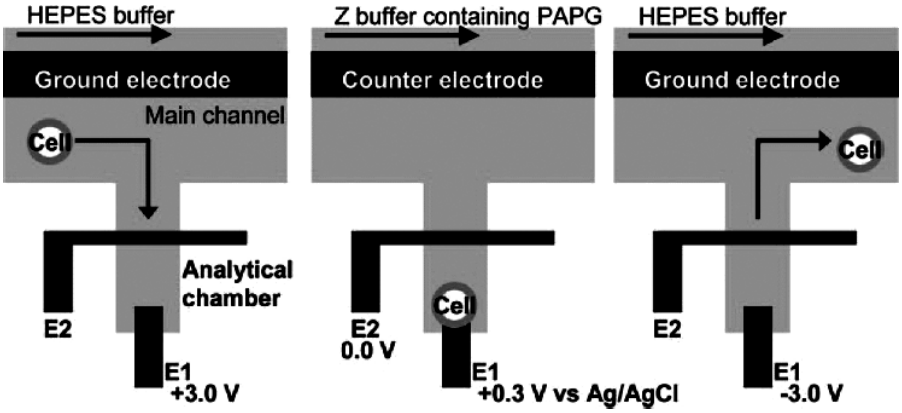

Fig. 1 Electrophoretic cell manipulation and electrochemical measurement in a microfluidic device. Reproduced from Ref. 48 with permission. Copyright 2008 American Chemical Society.

active modes. The passive mode makes use of the interactions between particles, between particles and microchannel structure, and between particles and flow. A number of concepts for particle separation based on the passive mode have been proposed; pinched flow fractionation,[10-13] inertia and dean flow fractionation,[14-18] microvortex manipulation,[19-22] deterministic lateral displacement,[6,23-26] Zweifach–Fung effect,[27-30] hydrodynamic chromatography,[31-36] and hydrodynamic filtration.[37-40] Passive-mode separation is well suited to a macro/nanofluidic device, in which complex channel structures can be constructed on a microchip and flows can be precisely managed.

In the active mode, an external physical field, including electric, dielectric, magnetic, flow, thermal, and acoustic field, creates the distribution of particles based on their physical property, such as size, shape, deformation, density, electronic charge, compressibility, permittivity, and magnetic susceptibility. The particle distribution allows the separation of particles, which flow down with different streamlines or at different rates. The separation efficiency of the active mode is generally higher than that of the passive mode. A representative separation principle of the active mode is field-flow fractionation (FFF), in which an external field is applied perpendicular to a fluid flow. Particles experience a force toward an accumulation wall by the physical field and simultaneously a diffusion force. Their elution from a separation channel is determined by the balance between these competing forces. Readers, who are interested in FFF, can find excellent reviews on this topic.[41-43]

An external field is effective not only for particle separation but also for its manipulation. A single particle or only a few particles are usually manipulated using an external field, whereas separation, in general, handles an ensemble of particles. Therefore, results of separation can be considered as the statistical compilation of single-particle behavior that are the subject of manipulation work studies. The results of manipulation can be straightforwardly discussed based on the theories of a physical field. Particle manipulation is utilized not only for trapping, transportation, and patterning of particles but also for the evaluation of their physicochemical properties and the reactions or interactions that occur on a particle. The present review focuses on particle manipulation using external physical fields and discusses its advantages and limitations.

2 Particle Manipulation with External Physical Fields

2·1 Electric field

An electric force (F_e) exerted on a particle carrying a charge of q is expressed by the following equation:

$$F_e = qE = 2\pi d_p\left(1 + \frac{1}{2}\kappa d_p\right)\varepsilon\zeta E \quad (1)$$

where d_p is the particle diameter, ζ is the zeta potential, and κ is the Debye–Hückel parameter given by:

$$\kappa = \sqrt{\frac{e^2 N_A}{\varepsilon kT}\sum_i (n_i z_i^2)} \quad (2)$$

where e is the elementary charge, N_A is the Avogadro number, ε is the permittivity of a medium, k is the Boltzmann constant, T is the temperature, n_i is the concentration of an ion (mol m^{-3}), and z_i is the ion valency. For example, a 4.5-μm polystyrene particle with a charge density of 1.8×10^{-6} C m^{-2} undergoes $F_e = 2.5 \times 10^{-13}$ N in $E = 50$ V m^{-1}.[44]

Analytical chemists are familiar with an electric field, which is, for example, explored in electrophoresis. Slab gel electrophoresis is a powerful tool in biomedical analyses. The exploitation of capillary electrophoresis (CE) inspired a number of analytical chemists to work on this method relying on an electric field. Now, CE expands its application from simple ions and molecules to biopolymers, bacteria, and particles.[45-47] When a charged particle is introduced to an electric field established along a capillary, it migrates to one of the electrodes, anode or cathode, depending on its effective charge, at an electrophoretic velocity (v_p):

$$v_p = \mu_p E \quad (3)$$

where μ_p is the electrophoretic mobility. The electric double layer (EDL) is formed near the inside wall of the silica capillary because of the negative charge of the silica wall arising from the dissociation of silanol groups. When an electric field is applied, cations accumulated in the EDL migrate toward the cathode. This migration causes a fluid flow in the same direction, which is called an electroosmotic flow. Thus, the apparent velocity of the particle is given by:

$$v_{app} = v_p + v_{EOF} \quad (4)$$

where v_{EOF} is the velocity of the electroosmotic flow. Because $v_{EOF} > v_p$ in many cases, particles flow out of the cathodic end irrespective of the signs of their charge.

Matsue *et al.* reported the electrophoretic manipulation of a single cell (Fig. 1).[48] A voltage of +3.0 V was applied to E1 electrode against the ground electrode in the main channel. A biological cell, which was introduced into the analytical chamber by a flow, was trapped on the electrode, where the β-galactosidase activity of the cell was monitored. After the measurement, the cell was released into the main channel by applying –3.0 V to the E1 electrode. This system allowed the sensitive electrochemical detection of enzyme activities at the single-cell level. Mesquida *et al.* manipulated multiple oil-in-water-in-oil (O/W/O) and water-in-oil-in-water-in-oil (W/O/W/O) emulsions by electrophoresis.[49] The electrophoreric mobility of an emulsion was determined solely by the charge and polarity of the outermost water layer regardless of their sizes and compositions. Shan *et al.* developed a device for manipulating multiple nanowires using an electric field.[50] An electrode array and a plate electrode were placed on the bottom and top of a microfluidic device, respectively. Multiple nanowires were manipulated at their disposal by switching active electrodes in the array.

Cohen *et al.* reported the electrokinetic trapping of nanoscale objects in a solution.[51] Four microelectrodes were fabricated on a slide glass as shown in Fig. 2. A particle with 200 nm diameter was entrapped at the center of the glass slide by electrophoresis. Yazbeck *et al.* proposed nanopore-based electrokinetic tweezers for manipulating and characterizing a single nanoparticle.[52] A voltage bias was applied across the nanopore. A charged nanoparticle simultaneously experienced F_e, F_{EOF}, and dielectrophoretic force (F_{DEP}) and was trapped at the position, where the three forces were balanced.

The electric field can recognize the surface property of particles, that is q, unlike other external fields that are selective to bulk properties. A substance usually has an intrinsic surface charge, which is often pH-dependent. Therefore, in solutions, any substance, from a molecule to a particle, undergoes F_e, and can be electrically manipulated. In addition, this approach has many other advantages, such as the rapid response, easy device construction, and high reproducibility. On the other hand, because an electric field acts over a wide range and all of the particles simultaneously experience an electric force, single particle manipulation and trapping is, in general, difficult. Thus, for single particle manipulation, an electric field is combined with other external fields or incorporated in a microfluidics device. Moreover, applications of an electric field are limited to conductive solvents, usually water, because an electric current cannot flow in poorly conductive media.

2·2 Dielectrophoresis

Dielectrophoresis (DEP), which was first described by Pohl, has recently been explored for the separation and manipulation of particles.[53,54] When a polarizable particle is placed in an ununiform electric field, it experiences an attractive or repulsive force. The time-averaged DEP force exerted on a homogeneous sphere is given by:[53-57]

$$\langle F_{DEP} \rangle = 2\pi r^3 \varepsilon_m \mathrm{Re}[f_{CM}(\omega)] \nabla |\vec{E}_{rms}|^2 \quad (5)$$

where r is the radius of the particle, ε_m is the permittivity of a medium, ∇ is the gradient operator, and E_{rms} is the root mean square electric field. $\mathrm{Re}[f_{CM}(\omega)]$ refers to the real component of

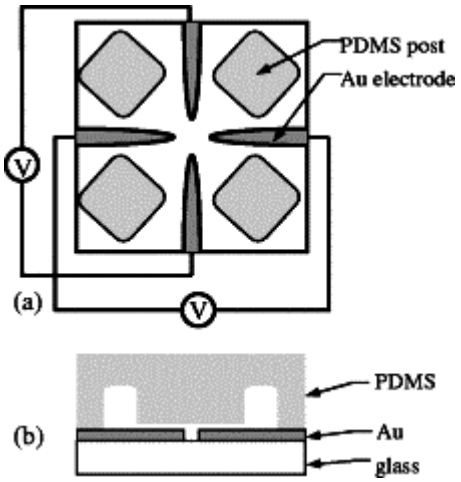

Fig. 2 Schematic representation of an electrokinetic trapping device, (a) top and (b) side views. Reproduced from Ref. 51 with permission. Copyright 2005 the American Institute of Physics.

Clausius–Mossotti (CM) factor:

$$\mathrm{Re}[f_{CM}(\omega)] = \frac{\varepsilon_p^* - \varepsilon_m^*}{\varepsilon_p^* + 2\varepsilon_m^*} \quad (6)$$

where ε_p^* and ε_m^* represent the complex permittivity of the particle and medium, respectively. Although for multi-shell spheres and non-spheres has also been derived,[54] we here discuss the DEP behavior of homogeneous spheres. $\langle F_{DEP} \rangle$ exerted on microparticles is in the nN range when E_{rms} = 1000 – 5000 V m^{-1}.[58]

A particle moves in the direction increasing electric field density (positive DEP) when $\mathrm{Re}[f_{CM}(\omega)] > 0$, while it moves in the opposite direction when $\mathrm{Re}[f_{CM}(\omega)] < 0$ (negative DEP). Figure 3 shows the relationship between the frequency of an electric field and $\mathrm{Re}[f_{CM}(\omega)]$, which was calculated for $\varepsilon_p^* < \varepsilon_m^*$. The $\mathrm{Re}[f_{CM}(\omega)]$ value changes from negative to positive in a sigmoidal fashion as the frequency increases. This indicates that the particles with different ε_p^* values can be separated by adjusting the frequency of an electric field.

Hund and Westervelt have developed DEP tweezers for manipulating a yeast cell.[59] The sharp glass tip with two electrodes on either side was used as the tweezers. When the voltage was applied between the electrodes, the electrically polarized yeast cell was entrapped at the tip. Takeuchi *et al.* improved this concept using round-tip DEP tweezers, which induce a high electric field density at the tip of the tweezers.[60] They selectively manipulated a labeled single cell in a number of unlabeled cells. Chou *et al.* proposed the electrodeless DEP trapping of single- and double-stranded DNA molecules using a constriction array.[61] The application of a voltage across the constructions induced a strong electric field at the orifice, where DNA molecules were trapped. Grom *et al.* succeeded in the entrapment of Hepatitis A virus particles by a combination of electrohydrodynamic flow and DEP force.[62] An electric field cage was constructed with eight electrodes at all corners of the cage. These electrodes generated a strong electric field at the center of the cage. In a highly conductive medium, Joule heating caused an electrohydrodynamic flow toward the center of the cage, where a DEP force trapped particles. Thus, the virus particles were stably retained at the center of the cage.

Significant advantages of DEP in the trapping and manipulation

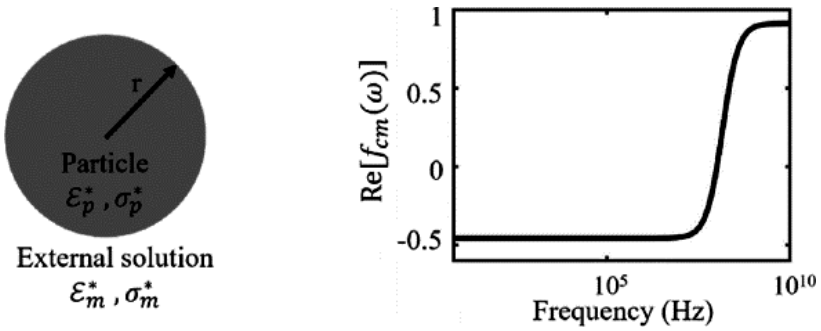

Fig. 3 Schematic representation of a homogeneous sphere and frequency dependence of Re[$f_{CM}(\omega)$] calculated for $\varepsilon_p^* < \varepsilon_m^*$. σ_m^* and σ_p^* represent the conductivity of the medium and particle, respectively. Reproduced from Ref. 55 with permission. Copyright 2019 American Chemical Society.

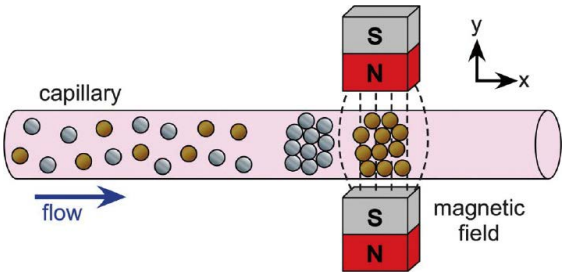

Fig. 4 Schematic representation of the simultaneous trapping of magnetic (brown) and diamagnetic particles (grey) in a paramagnetic medium. The magnetic particles, which have positive F_{mag}, are trapped between the magnets, while the diamagnetic particles (negative F_{mag}) are repelled from the field and are assembled at the position, where the flow (Stokes drag) and magnetic forces are balanced. Reproduced from Ref. 66 with permission. Copyright 2013 Royal Society of Chemistry.

of particles are: (1) applicability to targets with various sizes from molecules to microparticles, and (2) control of the particle movement direction by changing the electric field frequency. In actuality, various targets, such as cells, organelles, nucleic acids, proteins, and viruses, were successfully entrapped and manipulated.[2,54,55] DEP is effective for the selective trapping of one target from a mixture with another different target. However, the selective entrapment of a given one from more than two different targets is severely restricted because selectivity is determined by frequency; it is actually impossible to select an appropriate electric field frequency that effectively acts on only one target.

2·3 Magnetic field

A magnetic field is usually formed using a permanent magnet or an electromagnet. An inhomogeneous magnetic field exerts an attractive or repulsive force on a magnetic particle. The magnetic force is represented by the following equation:[5,7,56,63,64]

$$F_{mag} = \frac{4\pi r^3}{3}(\chi_m - \chi_p)\frac{(B\nabla)B}{\mu_0} \quad (7)$$

where χ_p and χ_m are the magnetic susceptibility of the particle and medium, respectively, B is the magnetic field intensity, and μ_0 is the magnetic permeability of vacuum. F_{mag} of ~ pN can be exerted on a particle using a small permanent magnet.[65]

Pamme *et al.* demonstrated the simultaneous capture of magnetic and diamagnetic particles based on the magnetophoretic principle (Fig. 4).[66] Positive F_{mag} acts on the former ($\chi_p > 0$) but negative F_{mag} on the latter ($\chi_p < 0$). Thus, the magnetic particles were trapped by the field, while the diamagnetic particles were expelled from the field and were assembled at a position where the Stokes drag and repulsive magnetic force were balanced. Alsberg *et al.* studied the magnetophoresis of cells covered by magnetic nanoparticles.[67] A magnetic force was exerted on the cells, which were linearly arranged by the negative magnetophoresis. The cells were transported along the field and adhered to each other by the strong intercellular interaction, which led to the alignment of the cells. Watarai *et al.* evaluated the adsorption of dysprosium(III) ion onto a single microdroplet containing *n*-alkylcarboxylic acid from the magnetophoretic behavior of the droplet. The magnetophoretic velocity of the droplet became larger due to the interfacial complexation of Dy(III), which changed χ_p.[68] Whitesides *et al.* developed a novel magnetic manipulation, called magnetic levitation (MagLev).[69–73] MagLev can recognize the density of a particle or a liquid droplet and levitate it at the coordinate, where the magnetic and sedimentation forces are balanced (Fig. 5).

Magnetic tweezers were also developed for particle manipulation.[74–76] Basic magnetic tweezers consisted of a permanent magnet placed above the sample holder, which was usually fitted on an inverted microscope (Fig. 6). The magnetic tweezers can exert a force of 10^{-3} – 10^2 pN on 0.5 – 5 µm paramagnetic particles.[75] This force is just in the same range as the intra and intermolecular forces. Therefore, the magnetic tweezers can cause the extension or contraction of molecules tethered to the magnetic particles. This technique was applied to the mechanochemical studies of DNA gyrase[77] and a rotary motor enzyme, F_0F_1ATPase.[78] Recently, Popa *et al.* used the magnetic tweezers to evaluate the folding/unfolding dynamics of proteins.[79] A magnetic particle was anchored on a substrate through a chain of eight target protein molecules. The magnetic force of 100 pN was repeatedly applied to the particle to induce the unfolding-refolding cycles of the protein chain in the absence or presence of a ligand. They found that the ligand binding enhances the mechanical strength of the protein at the unfolding state. Harada *et al.* visualized the DNA rotation during the transcription by RNA polymerase using a real-time optical microscopy combined with the magnetic tweezers, where the DNA molecule was anchored on a magnetic bead.[80]

A magnetic field allows the simple design of experimental systems for the manipulation of particles, because a magnetic field is easily formed using a permanent magnet or an

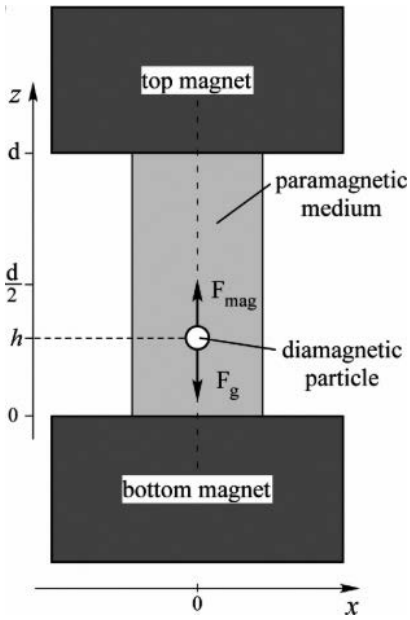

Fig. 5 Conceptual scheme of MagLev. A diamagnetic particle immersed in a paramagnetic medium is placed between a pair of magnets. A magnetic force (F_{mag}) exerted on the particle competes with the sedimentation force (F_g). The magnetic particle is levitated at the position where two forces are balanced. Reproduced from Ref. 72 with permission. Copyright 2009 American Chemical Society.

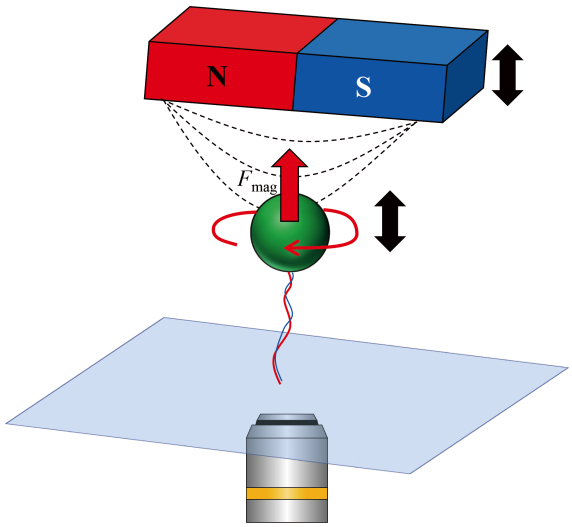

Fig. 6 Schematic representation of magnetic tweezers.

electromagnet and selectively recognizes magnetic particles from nonmagnetic ones. The magnetic field is suitable for the separation and manipulation of multiple particles because it acts over a large distance. On the other hand, its application is limited to the trapping and manipulation of magnetic particles and ferrofluid. Therefore, biological samples, such as cells and organisms, should be modified by magnetic materials for manipulation. Although MagLev is a label-free technique, particle manipulation has not been accomplished using this technique. In addition, its application is limited to millimeter- or submillimeter-sized particles because of the slow response of smaller particles.

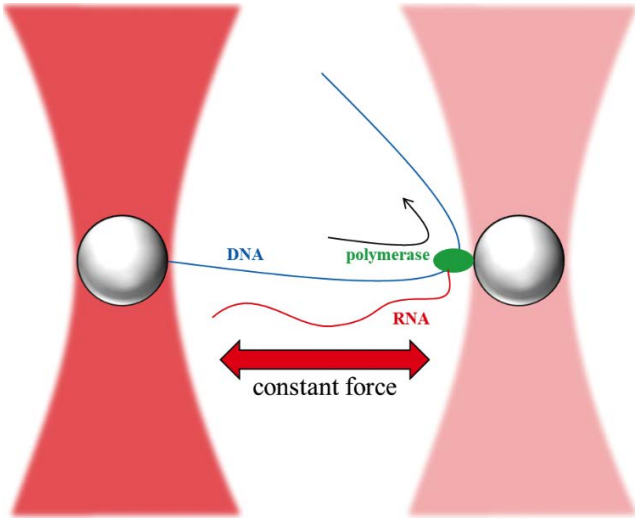

Fig. 7 Visualization of RNA polymerase translocation using optical trapping. Two beads (gray) are trapped by optical fields (pink). A DNA molecule (blue) and enzyme (green) are anchored on the left and right beads, respectively. DNA is transcribed into RNA (red) by RNA polymerase. As the transcription proceeds, the right bead, which is weakly trapped, approaches the strongly trapped left bead.

2·4 Optical field

The passage of the light through a substance causes a change in the light momentum because of the refraction of the light. Because the total amount of the momentum should be conserved, the substance experiences an optical force (F_{opt}) represented by:[81,82]

$$F_{opt} = \frac{2n_1P}{c}\left(\frac{r}{\omega}\right)^2 Q^* \quad (8)$$

where n_1 is the refractive index of the medium, P is the laser power, c is the speed of the light, and Q^* is the trapping efficiency that depends on the size, shape, material of the substance, and its position with respect to the spatial profile of the light. For spherical particles with diameters of 0.25 – 5 μm, the optical force typically ranges from 0.1 to 100 pN.[74,80] The principle was established by Ashkin,[83] who won the Nobel Prize in Physics in 2018. He showed that a particle with a higher refractive index than a medium is attracted to the center of a laser beam. This technique was applied to spectroscopic and electrochemical measurements of a single microdroplet[84–88] and an optical trapping of amino acids and proteins.[89,90]

Optical tweezers trap and manipulate particles and cells based on this principle. For example, Reid *et al.* demonstrated the stable trapping of aerosol by a vertically or horizontally propagating laser beam.[91] Abbondanzieri *et al.* revealed the mechanism of RNA polymerase translocation using dual optical tweezers, which individually trapped a DNA-anchored bead and an RNA polymerase-anchored bead at different positions by different forces.[92] As shown in Fig. 7, one bead was strongly trapped, while the other was weakly trapped. Therefore, the location of the weakly trapped particle was shifted as the polymerase translocation proceeded. From the dynamic movement of the bead, a discrete step was determined to be 3.7 ± 0.6 Å, which corresponded to the length of one base in a DNA molecule. Thus, they succeeded in the direct observation of the step-by-step translocation of RNA polymerase by this approach. Ritsch-Marte *et al.* designed “macro-tweezers” for

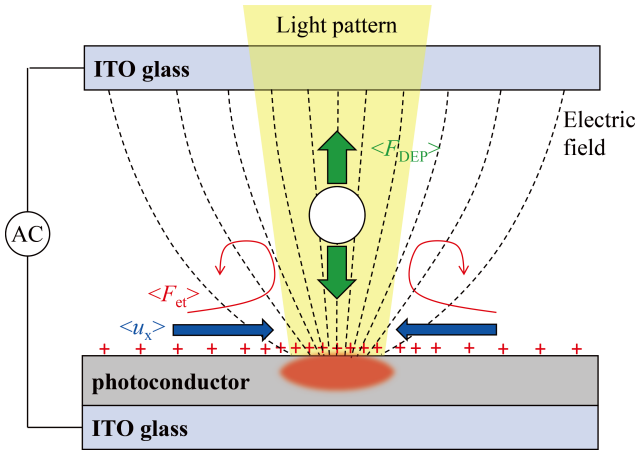

Fig. 8 Schematic representation of the principle POT. When the light emits on the photoconductor substrate, ununiform electric field and heat are induced, resulting in the generation of $\langle F_{DEP}\rangle$, $\langle F_{et}\rangle$, and $\langle u_x\rangle$.

trapping highly motile organisms.[93] Two beams are coaxially irradiated but focuses on different focal points. Organisms with 70 µm length, which were not captured using a single beam, were successfully trapped between two focal points.

Optoelectronic tweezers (OETs) are a novel optical manipulation tool.[94-96] Figure 8 shows the principle of OETs. Light illumination on a photoconductor substrate induces a ununiform electric field, which causes DEP, AC electroosmosis (ACEO), and an electrothermal flow. When an electrode is in contact with an electrolyte solution, an EDL is formed near the electrode. This EDL is tangentially formed in the light-illuminated region. The counterions migrate along a potential gradient induced by the light irradiation, which causes an EOF-driven vortex. The time-averaged ACEO flow velocity ($\langle u_x\rangle$) is given by:[95]

$$\langle u_x\rangle = \frac{1}{2}\mathrm{Re}\left[\frac{\sigma_q E_t^*}{\kappa\eta}\right] \tag{9}$$

where σ_q is the charge density in the EDL, E_t^* is the complex conjugate of the electric field induced by the light, and η is the viscosity of the medium. The irradiation of an infrared laser beam on the surface of an ITO electrode causes heating and induces an electrothermal flow. A time-averaged electrothermal force ($\langle F_{et}\rangle$) is represented by:[95]

$$\langle F_{et}\rangle = \frac{1}{2}\mathrm{Re}\left[\left(\frac{(\sigma\nabla\varepsilon - \varepsilon\nabla\sigma)E}{\sigma + i\omega\varepsilon}\right)E^* - \frac{1}{2}|E|^2\nabla\varepsilon\right] \tag{10}$$

where ω is the angular frequency of the AC electric field, σ and ε is the conductivity and permittivity of the medium. These three effects (DEP, ACEO and electrothermal flow) help trap particles and macromolecules on the substrate surface.

Wu *et al.* developed a novel OET device for cell manipulation using a spatial light modulator, which arbitrarily generated dynamic manipulation patterns.[97] The OET device consisted of an upper ITO electrode and a lower electrode with a photoconductive layer. Particle suspension was sandwiched between these two electrodes. When the patterned project light, which is hollow square, is irradiated onto the photoconductor, a particle inside the pattern experiences an optically induced negative DEP force. Since the projection pattern can be arbitrarily varied, not only the dynamic manipulation but also the simultaneous trapping of multiple particles or cells is possible. Neale *et al.* proposed measurements of the relative stiffness of murine erythrocytes using OET.[98] In this system, nonspherical cells were aligned and stretched along an electric field. Changes in the diameter of murine erythrocytes were measured to characterize the cell stiffness.

An optical field is particularly suitable for the trapping and manipulation of a single particle or cell because an optical force can be focused on a small space. Moreover, F_{opt} is proportional to the square of the particle radius as shown by Eq. (8). This suggests that the optical field can handle small particles that cannot be captured by other fields, where the force is a function of the cube of the particle radius. However, because the difference in the refractive index between a particle and medium is a critical parameter for optical trapping, the trapping of a biological sample in water is, in general, difficult because of a low refractive index contrast. Therefore, high concentrations of a solute such as sucrose are often required to increase the refractive index difference between the medium and targets. In addition, the optical trapping of multiple particles is difficult because an optical force acts on the particles just around the light. Although these disadvantages have been partly overcome by OET, the complex instrumental setup is a problem for its wider application.

2·5 Plasmonic optical tweezers

Optical tweezers have its intrinsic limitation that nano-sized materials or molecules cannot be directly trapped. A novel optical manipulation technique called plasmonic optical tweezers (POT) has recently been developed to overcome this limitation.[99] A metal nanoparticle or metal thin layer is illuminated with light to cause surface plasmon resonance (SPR), which generates an intense electromagnetic field near the metal surface. An optical force induced by the electromagnetic field is expressed by:[100,101]

$$\langle F_{oe}\rangle = \int_{\partial V}\langle T(r,t)\rangle n da \tag{11}$$

where ∂V is the surface of a volume enclosing an irradiated structure and T is the Maxwell stress tensor. When a particle radius, a, is smaller than the wavelength and the length of the electromagnetic field, the particle is regarded as a point dipole, and the optical gradient force (F_{POT}) becomes dominant:

$$F_{POT} = \frac{2\pi\alpha}{cn_1^2}\nabla I_0 \tag{12}$$

where I_0 is the intensity distribution of the electromagnetic field and α is the polarizability of the particle, which is given by:

$$\alpha = n_1^2 a^3 \frac{(n_2/n_1)^2 - 1}{(n_2/n_1)^2 + 2} \tag{13}$$

where n_2 is the refractive index of the particle. A force from POT efficiently acts even on a nanoparticle (>10 nm).[4]

Yang *et al.* demonstrated the transport and trapping of nanospheres using a two-dimensional plasmonic optical lattice of gold nanostructures. Nanoparticles were assembled at the center of the array to form a hexagonal closed pack crystalline structure, as shown in Fig. 9.[102] Tsuboi *et al.* reported the switchable POT trapping of DNA molecules based on localized surface plasmon using NIR laser irradiation.[103] A continuous laser irradiation generated not only an enhanced electromagnetic field but also heat around the nanostructure, causing

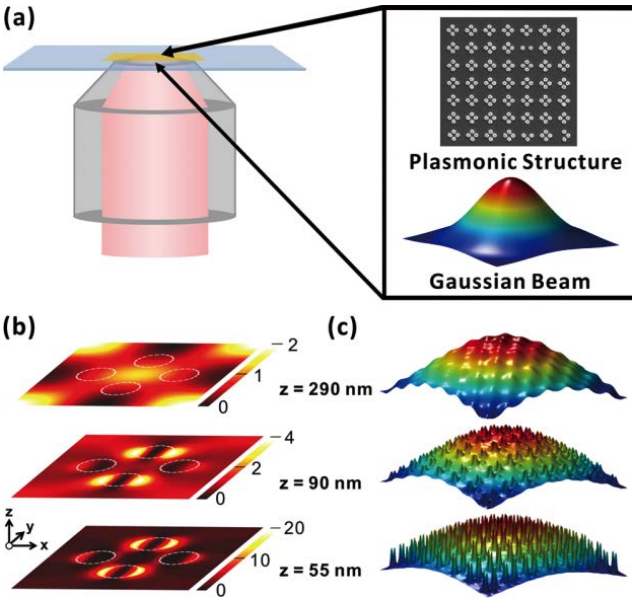

Fig. 9 (a) Microscope setup and two-dimensional plasmonic optical lattice of gold nanostructure. Simulated intensity distribution of time-averaged electric field (b) and intensity profiles on the optical lattice at various planes above the substrate (c). Reproduced from Ref. 102 with permission. Copyright 2013 American Chemical Society.

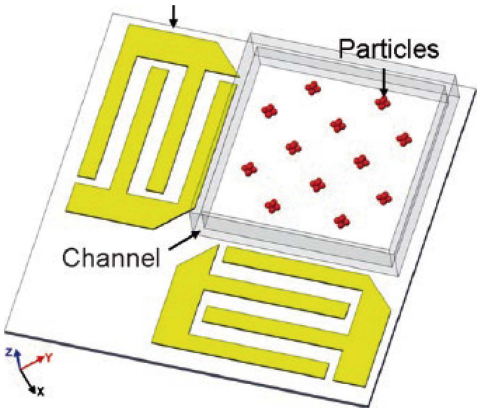

Fig. 10 Schematic representation of 2D patterning of particles. Two IDTs are orthogonally arranged. Reproduced from Ref. 108 with permission. Copyright 2009 Royal Society of Chemistry.

thermophoresis of DNA. DNA molecules were aggregated on a metallic nanostructure by an optical force and thermophoresis. Yoon *et al.* used a bowtie nanostructure, which generated SPR between two sharp tips, for trapping a single sub-5 nm particle.[104] A quantum dot was trapped between the tips and detected as an optical spike on the enhanced second harmonic signal.

POT has the following advantages over the conventional optical tweezers. First, the laser intensity used in POT is lower than that required for conventional optical tweezers because the electromagnetic field can be enhanced by plasmon in the former. Second, the spatial resolution is so high that the motion of the trapped particle can be precisely controlled in plasmonic nanospace. Third, nanoparticles and macromolecules can be manipulated. Finally, POT can be combined with conventional other methods such as photochemical reactions and highly sensitive chemical and biological sensors. However, the mechanism of POT remains unclear because it involves photothermal effects caused by plasmon excitation, which has not been theoretically formulated. Thus, further experimental and theoretical studies are necessary.

2·6 Acoustic field

Ultrasound is also used for the separation and manipulation of particles. In an acoustic standing wave field, particles experience an acoustic radiation force (F_{ac}), which is given by the following equations:[5,56,57,105-107]

$$F_{ac} = -\frac{4}{3}\pi r^3 k E_{ac} A \sin(2kz) \tag{14}$$

$$A = \frac{5\rho^* - 2\rho}{2\rho^* + \rho} - \frac{\rho c^2}{\rho^* c^{*2}} = \frac{5\rho^* - 2\rho}{2\rho^* + \rho} - \frac{\gamma^*}{\gamma} \tag{15}$$

$$E_{ac} = \alpha V^2 \tag{16}$$

where k is the wavenumber of the ultrasound, z is the distance from the node or antinode of the standing wave, α is the device-dependent parameter, V is the voltage applied to an ultrasound transducer, and ρ and γ are the density and compressibility of a medium (asterisk represents a particle), respectively. A particle moves toward the antinode of the standing wave when $A < 0$, whereas positive A predicts its movement toward the node. Since these equations are applicable to spherical particles, modifications are necessary to describe the acoustic force on nonspheres.

Huang *et al.* reported the patterning of cells and microparticles using two orthogonally arranged interdigital transducers (IDTs), as illustrated in Fig. 10.[108] The particles are aggregated at the intersections of two nodal lines. Benkovic *et al.* demonstrated the on-chip manipulation of a single microparticle using a surface-acoustic wave device, in which pairs of chirped IDTs were orthogonally arranged to generate 2D standing wave patterns.[109] A particle, which moved with the node, was manipulated by controlling the resonance frequency of the chirped IDT. Zheng *et al.* demonstrated the destruction of a microbubble cluster at a desired location to achieve a single cell sonoporation using a phase-shift method.[110] A microbubble cluster was translocated to approach a target cell by managing the phase of the untrasound. Its collapse near the cell caused sonoporation with high efficiency.

A single particle trapping with an acoustic field has been performed based on various concepts. Thomas *et al.* theoretically and experimentally demonstrated the trapping of a single elastic particle with a focused acoustic beam.[111] The particle was levitated at the position where the sedimentation, drag, and radiation forces were balanced. This allowed the precise trapping and manipulation of a single particle. Poulikakos *et al.* showed the levitation and rotation of polystyrene particles and droplets using multiphase transducers, where three pairs of ultrasound emitter and reflector were triangularly placed.[112] A particle was trapped at the center of the three emitter-reflector pairs. The ultrasound phase shift caused the rotation of the particle. We evaluated the ion-exchange reaction occurring in a single resin bead, which was levitated in a coupled acoustic-gravitational (CAG) field.[113] The levitation coordinate of the bead is a function of its acoustic properties such as density and compressibility. Because these properties of the resin are determined by the nature of a counterion, the ion-exchange reaction in the resin bead causes a change in the levitation coordinate. The equilibrium and kinetics of the ion-

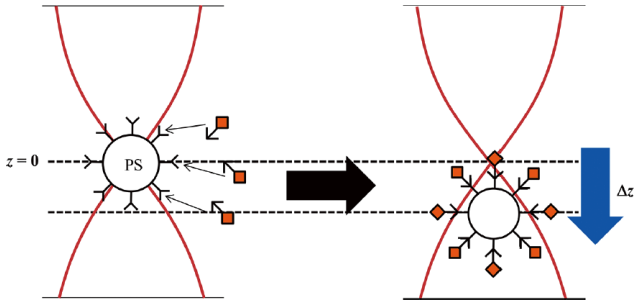

Fig. 11 Main conceptual scheme for a trace analysis based on a levitation coordinate shift using the CAG field. When gold nanoparticles (AuNPs) are bound to a microparticle through a surface reaction, the density of AuNP-bound microparticle increases, which leads to levitation coordinate change. The difference in the coordinate allows us to determine the number of bound AuNP. If a target mediates the interparticle reaction, we can determine the target concentration from the coordinate shift of the microparticle. Reproduced from Ref. 117 with permission. Copyright 2018 American Chemical Society.

exchange reaction were evaluated by this approach. We also developed trace bioanalysis schemes based on the levitation coordinate shifts of a single microparticle in the CAG field.[114-118] The main concept is illustrated in Fig. 11. Since the density of a microparticle increases by the binding of gold nanoparticles (AuNPs), we can determine the number of AuNPs bound to the microparticle from the shift of its levitation coordinate. Because various reactions of biochemical importance can be incorporated to mediate the binding between microparticles and AuNPs, this scheme allowed us to detect targets, such as protein, DNA, RNA, and physiologically active substances, at the zmol level.

An acoustic field has several advantages over other physical fields in particle trapping and manipulation. The acoustic field is applicable to a variety of media, such as gas, aqueous solutions, and organic solvents. This is a good contrast to other physical fields, which often require special properties of media for successful particle manipulation. Also, an acoustic radiation force does not cause damage to biological cells unlike ultrasonic cavitation. Therefore, this field can also be employed for manipulating biological samples. On the other hand, the acoustic field has some weak points. An observation cell should be fabricated using homogenous materials with precisely adjusted sizes to maintain an appropriate resonance condition, which enables the generation of a well-defined ultrasound standing wave and, as a result, stable trapping of particles. Moreover, the acoustic field is inapplicable to nanoparticles because the F_{ac} is a function of the particle volume and rapidly becomes weak as the particle size decreases. Although the use of high frequency may help trap smaller particles, we would encounter other difficulties in the precise fabrication of a tiny observation cell and the interference from an ultrasound stream.

3 Conclusions and Perspectives

The external fields provide versatile ways not only for the trapping and manipulation of particulate targets but also for evaluating their physical properties, interactions, and reactions. Each external field has its own advantages and disadvantages. One of the common problems that we often encounter during work on the manipulation of particles is the Brownian motion. The external force should always compete with and conquer the Brownian force to attain stable manipulation. In particular, when nano or submicron particles are handled, this effect becomes dominant and renders manipulation difficult. Forces effectively acting on particles with such small dimensions should be developed for further application of external fields to nanomaterials.

A number of studies have indicated that external fields are highly compatible with microfluidic devices. One of the advantages of microfluidics is the facile fabrication of complicated channel structures, which could not be attained without this technique. The external force can be sufficiently exerted on targets in the microfluidic devices to allow efficient trapping and manipulation of particles. External fields, which are integrated on microfluidic devices, are successfully used for drug delivery, biosensing, and imaging.

The combination of multiple external fields also facilitates versatile applications. For example, Whitesides *et al.* developed MagLev, where the magnetic field was combined with the gravitational field, for determining particle density.[72] We also developed the CAG field for density-based sensing and separation.[119] OET intrinsically utilizes combined fields. Thus, the efficient combination of multiple external fields has further potential for developing novel schemes.

As stated above, most of the physical forces cannot be directly exerted on nanoparticles or molecules. However, targets of such small dimensions can be indirectly characterized by observing the behavior of a microparticle in an external field. In such studies, small targets are bound to a microparticle, which is manipulated by an external force. The reactions and interactions of targets influence the behavior of the microparticles in the force field and are indirectly detected as *e.g.* a shift of the location of a trapped particle. This approach has high potential particularly for studies of biomolecules. We believe that particle manipulation in external physical fields continues to make great contributions to the advancements of a wide variety of disciplines, particularly in bioscience, biotechnologies, and materials science.

4 References

1. M. Li, W. H. Li, J. Zhang, G. Alici, and W. Wen, *J. Phys. D: Appl. Phys.*, **2014**, *47*, 063001.
2. M. R. Buyong, A. A. Kayani, A. A. Hamzah, and M. B. Yeop, *Biosensors (Basel)*, **2019**, *9*, 30.
3. X. Lu, C. Liu, G. Hu, and X. Xuan, *J. Colloid Interface Sci.*, **2017**, *500*, 182.
4. A. Ozcelik, J. Rufo, F. Guo, Y. Gu, P. Li, J. Lata, and T. J. Huang, *Nat. Methods*, **2018**, *15*, 1021.
5. P. Sajeesh and A. K. Sen, *Microfluid. Nanofluid.* **2014**, *17*, 1.
6. J. McGrath, M. Jimenez, and H. Bridle, *Lab Chip*, **2014**, *14*, 4139.
7. L. Borlido, A. M. Azevedo, A. C. A. Roque, and M. R. Aires-Barros, *Biotechnol. Adv.*, **2013**, *31*, 1374.
8. S. Li, F. Ma, H. Bachman, C. E. Cameron, X. Zeng, and T. J. Huang, *J. Micromech. Microeng*, **2017**, *27*, 015031
9. C. W. Shields IV, C. D. Reyes, and G. P. López, *Lab Chip*, **2015**, *15*, 1230
10. J. Oakey, J. Alley, and D. W. M. Marr, *Biotechnol. Prog.*, **2002**, *18*, 1439.
11. M. Yamada, M. Nakashima, and M. Seki, *Anal. Chem.*, **2004**, *76*, 5465.
12. A. L. Vig and A. Kristensen, *Appl. Phys. Lett.*, **2008**, *93*, 203507.
13. R. Zhou and C. Wang, *J. Micromech. Microeng.*, **2015**, *25*,

084005.
14. J.-S. Park and H.-I. Jung, *Anal. Chem.*, **2009**, *81*, 8280.
15. S. C. Hur, N. K. Henderson-MacLennan, E. R. B. McCabe, and D. D. Carlo, *Lab Chip*, **2011**, *11*, 912.
16. M. G. Lee, S. Choi, and J.-K. Park, *J. Chromatogr. A*, **2011**, *1218*, 4138.
17. X. Lu and X. Xuan, *Anal. Chem.*, **2015**, *87*, 4560.
18. M. Masaeli, E. Sollier, H. Amini, W. Mao, K. Camacho, N. Doshi, S. Mitragotri, A. Alexeev, and D. D. Carlo, *Phys. Rev. X*, **2012**, *2*, 031017.
19. C.-H. Hsu, D. D. Carlo, C. Chen, D. Irimia, and M. Toner, *Lab Chip*, **2008**, *8*, 2128.
20. C.-H. Hsu, D. D. Carlo, C. Chen, D. Irimia, and M. Toner, *Proc. MicroTAS 2008*, **2008**, *12*, 1211.
21. T. Petit, L. Zhang, K. E. Peyer, B. E. Kratochvil, and B. J. Nelson, *Nano Lett.*, **2012**, *12*, 156.
22. D. T. Chiu, *Anal. Bioanal. Chem.*, **2007**, *387*, 17.
23. B. R. Long, M. Heller, J. P. Beech, H. Linke, H. Bruus, and J. O. Tegenfeldt, *Phys. Rev. E*, **2008**, *78*, 046304.
24. J. A. Davis, D. W. Inglis, K. J. Morton, D. A. Lawrence, L. R. Huang, S. Y. Chou, J. C. Sturm, and R. H. Austin, *Proc. Natl. Acad. Sci. U. S. A.*, **2006**, *40*, 14779.
25. H. Okano, T. Konishi, T. Suzuki, T. Suzuki, S. Ariyasu, S. Aoki, R. Abe, and M. Hayase, *Biomed. Microdevices*, **2015**, *17*, 59.
26. M. Heller and H. Bruus, *J. Micromech. Microeng.*, **2008**, *18*, 075030.
27. S. Yang, A. Ündar, and J. D. Zahn, *Lab Chip*, **2006**, *6*, 871.
28. H. W. Hou, H. Y. Gan, A. A. Bhagat, L. D. Li, C. T. Lim, and J. Han, *Biomicrofluidics*, **2012**, *6*, 024115.
29. Z. Fekete, P. Nagy, G. Huszka, F. Tolner, A. Pongrácz, and P. Fürjes, *Sens. Actuators, B*, **2012**, *162*, 89.
30. Z. Shen, G. Coupier, B. Kaoui, B. Polack, J. Harting, C. Misbah, and T. Podgorski, *Microvasc. Res.*, **2016**, *105*, 40.
31. T. Okada, *J. Liq. Chromatogr. Relat. Technol.*, **2010**, *33*, 1116.
32. R. Umehara, H. Miyahara, A. Okino, M. Harada, and T. Okada, *Anal. Sci.*, **2012**, *28*, 359.
33. R. Umehara, M. Harada, and T. Okada, *J. Sep. Sci.*, **2009**, *32*, 472.
34. M. Harada, T. Kido, T. Masudo, and T. Okada, *Anal. Sci.*, **2005**, *21*, 491.
35. T. Okada, M. Harada, and T. Kido, *Anal. Chem.*, **2005**, *77*, 6041.
36. T. Okada, "*Liquid Chromatography—Hydrodynamic Chromatography*", "*Encyclopedia of Analytical Science*", ed. P. Worsfold, D. Poole, A. Townshend, and M. Miro, 3rd ed., **2019**, Vol. 6, Elsevier, 93.
37. D. R. Gossett, W. M. Weaver, A. J. Mach, S. C. Hur, H. T. K. Tse, W. Lee, H. Amini, and D. D. Carlo, *Anal. Bioanal. Chem.*, **2010**, *397*, 3249.
38. V. VanDelinger and A. Groisman, *Anal. Chem.*, **2007**, *79*, 2023.
39. M. Matsuda, M. Yamada, and M. Seki, *Electron. Commun. Jpn.*, **2011**, *94*, 1.
40. R. Aoki, M. Yamada, M. Yasuda, and M. Seki, *Microfluid. Nanofluid.*, **2009**, *6*, 571.
41. M. I. Malik and H. Pasch, *Prog. Polym. Sci.*, **2016**, *63*, 42.
42. T. K. Mudalige, H. Qu, D. V. Haute, S. M. Ansar, and S. W. Linder, *TrAC, Trends Anal. Chem.*, **2018**, *106*, 202.
43. C. Contado, *Anal. Bioanal. Chem.*, **2017**, *409*, 2501.
44. K. Wada, K. Sasaki, and H. Masuhara, *Appl. Phys. Lett.*, **2002**, *81*, 1768
45. L. Kremser, D. Blaas, and E. Kenndler, *Electrophoresis*, **2004**, *25*, 2282.
46. S. P. Radko and A. Chrambach, *Electrophoresis*, **2002**, *23*, 1957.
47. N. Surugau and P. L. Urban, *J. Sep. Sci.*, **2009**, *32*, 1889.
48. T. Yasukawa, K. Nagamine, Y. Horiguchi, H. Shiku, M. Koide, T. Itayama, F. Shiraishi, and T. Matsue, *Anal. Chem.*, **2008**, *80*, 3722.
49. A. M. Schoeler, D. N. Josephides, A. S. Chaurasia, S. Sajjadi, and P. Mesquida, *Appl. Phys. Lett.*, **2014**, *104*, 074104.
50. K. Yu, J. Yi, and J. Shan, *IEEE Trans. Auto. Sci. Eng.*, **2018**, *15*, 80.
51. A. D. Cohen and W. E. Moerner, *Appl. Phys. Lett.*, **2005**, *86*, 093109.
52. R. Yazbeck, M. A. Alibakhshi, J. Von Schoppe, K. L. Ekinci, and C. Duan, *Nanoscale*, **2019**, *11*, 22924.
53. P. R. C. Gascoyne and J. Vykoukal, *Electrophoresis*, **2002**, *23*, 1973.
54. C. Zhang, K. Khoshmanesh, A. Mitchell, and K. Kalantar-Zadeh, *Anal. Bioanal. Chem.*, **2010**, *396*, 401.
55. D. Kim, M. Sonker, and A. Ros, *Anal. Chem.*, **2019**, *91*, 277.
56. A. Lenshof and T. Laurell, *Chem. Soc. Rev.*, **2010**, *39*, 1203.
57. M. Tenje, A. Fornell, M. Ohlin, and J. Nilsson, *Anal. Chem.*, **2018**, *90*, 1434.
58. K. Oshii, J. Choi, H. Obara, and M. Takei, *Journal of JSEM*, **2010**, *10*, 79.
59. T. P. Hunt and R. M. Westervelt, *Biomed. Microdevices*, **2006**, *8*, 227.
60. T. Kodama, T. Osaki, R. Kawano, K. Kamiya, N. Miki, and S. Takeuchi, *Biosens. Bioelectron.*, **2013**, *47*, 206.
61. C.-F. Chou, J. O. Tegenfeldt, O. Bakajin, S. S. Chan, E. C. Cox, N. Darnton, T. Duke, and R. H. Austin, *Biophys. J.*, **2002**, *83*, 2170.
62. F. Grom, J. Kentsch, T. Müller, T. Schnelle, and M. Stelzle, *Electrophoresis*, **2006**, *27*, 1386.
63. C. T. Yavuz, A. Prakash, J. T. Mayo, and V. L. Colvin, *Chem. Eng. Sci.*, **2009**, *64*, 2510.
64. M. Iranmanesh and J. Hulliger, *Chem. Soc. Rev.*, **2017**, *46*, 5925.
65. E. Brouzes, T. Kruse, R. Kimmerling, and H. H. Strey, *Lab Chip*, **2015**, *15*, 908.
66. M. D. Tarn, S. A. Peyman, and N. Pamme, *RSC Adv.*, **2013**, *3*, 7209.
67. M. D. Kreb, R. M. Erb, B. B. Yellen, B. Samanta, A. Bajaj, V. M. Rotello, and E. Alsberg, *Nano Lett.*, **2009**, *9*, 1812.
68. M. Suwa and H. Watarai, *Anal. Sci.*, **2008**, *24*, 133.
69. S. Ge and G. M. Whitesides, *Anal. Chem.*, **2018**, *90*, 12239.
70. A. Nemiroski, A. A. Kumar, S. Soh, D. V. Harburg, H. D. Yu, and G. M. Whitesides, *Anal. Chem.*, **2016**, *88*, 2666.
71. S. Ge, S. N. Semenov, A. A. Nagarkar, J. Milette, D. C. Christodouleas, L. Yuan, and G. M. Whitesides, *J. Am. Chem. Soc.*, **2017**, *139*, 18688.
72. K. A. Mirica, S. S. Shevkoplyas, S. T. Phillips, M. Gupta, and G. M. Whitesides, *J. Am. Chem. Soc.*, **2009**, *131*, 10049.
73. D. K. Bwambok, M. M. Thuo, M. B. Atkinson, K. A. Mirica, N. D. Shapiro, and G. M. Whitesides, *Anal. Chem.*, **2013**, *85*, 8442.
74. I. De Vlaminck and C. Dekker, *Annu. Rev. Biophys.*, **2012**, *41*, 453.
75. K. C. Neuman and A. Nagy, *Nat. Methods*, **2008**, *5*, 491.
76. F. Mosconi, J. F. Allemand, and V. Croquette, *Rev. Sci. Instrum.*, **2011**, *82*, 034302.
77. J. Gore, Z. Bryant, M. D. Stone, M. Nöllman, N. R.

Cozzarelli, and C. Bustamante, *Nature*, **2006**, *439*, 100.
78. H. Itoh, A. Takahashi, K. Adachi, H. Noji, R. Yasuda, M. Yoshida, and K. Kinosita Jr, *Nature*, **2004**, *427*, 465.
79. N. Dahal, J. Nowitzke, A. Eis, and I. Popa, *J. Phys. Chem. B*, **2020**, *124*, 3283.
80. Y. Harada, O. Ohara, A. Takatsuki, H. Itoh, N. Shimamoto, and K. Kinosita Jr, *Nature*, **2001**, *409*, 113.
81. A. Jonáš and P. Zemánek, *Electrophoresis*, **2008**, *29*, 4813.
82. K. Dholakia, M. P. MacDonald, P. Zemánek, and T. Čižmár, *Methods Cell Biol.*, **2007**, *82*, 467.
83. A. Ashkin, *Phys. Rev. Lett.*, **1970**, *24*, 156.
84. S. Ishizaka, T. Wada, and N. Kitamura, *Chem. Phys. Lett.*, **2011**, *506*, 117.
85. S. Ishizaka, K. Yamauchi, and N. Kitamura, *Anal. Sci.*, **2013**, *29*, 1123.
86. M. Uraoka, K. Maegawa, and S. Ishizaka, *Anal. Chem.*, **2017**, *89*, 12866.
87. K. Chikama, K. Nakatani, and N. Kitamura, *Chem. Lett.*, **1996**, *25*, 665.
88. K. Nakatani, M. Sudo, and N. Kitamura, *J. Phys. Chem., B*, **1998**, *102*, 2908.
89. Y. Tsuboi, T. Shoji, M. Nishino, S. Masuda, K. Ishimori, and N. Kitamori, *Appl. Surf. Sci.*, **2009**, *255*, 9906.
90. Y. Tsuboi, T. Shoji, and N. Kitamura, *J. Phys. Chem. C*, **2010**, *114*, 5589.
91. K. J. Knox, D. R. Burnham, L. I. McCann, S. L. Murphy, D. McGloin, and J. P. Reid, *J. Opt. Soc. Am. B*, **2010**, *27*, 582.
92. E. A. Abbondanzieri, W. J. Greenleaf, J. W. Shaevitz, R. Landick, and S. M. Block, *Nature*, **2005**, *438*, 460.
93. G. Thalhammer, R. Steiger, S. Bernet, and M. Ritsch-Marte, *J. Opt.*, **2011**, *13*, 044024.
94. M. C. Wu, *Nat. Photonics*, **2011**, *5*, 322.
95. A. Mishra, J.-S. Kwon, R. Thakur, and S. Wereley, *Trends Biotechnol.*, **2014**, *32*, 414.
96. H. Hwang and J.-K. Park, *Lab Chip*, **2011**, *11*, 33.
97. A. T. Ohta, P.-Y. Chiou, T. H. Han, J. C. Liao, U. Bhardwaj, E. R. B. McCabe, F. Yu, R. Sun, and M. C. Wu, *J. Microelectromech. Syst.*, **2007**, *16*, 491.
98. K. Dholakia, S. L. Neale, G. C. Spalding, N. Mody, C. Selman, and J. M. Cooper, *Proc. SPIE*, **2012**, *8458*, 845827.
99. A. N. Grigorenko, N. W. Roberts, M. R. Dickinson, and Y. Zhang, *Nat. Photonics*, **2008**, *2*, 365.
100. J.-S. Huang and Y.-T. Yang, *Nanomaterials (Basel)*, **2015**, *5*, 1048.
101. X. Han and C. Sun, *Appl. Sci.*, **2019**, *9*, 3596.
102. K.-Y. Chen, A.-T. Lee, C.-C. Hung, J.-S. Huang, and Y.-T. Yang, *Nano Lett.*, **2013**, *13*, 4118.
103. T. Shoji, J. Saitoh, N. Kitamura, F. Nagasawa, K. Murakoshi, H. Yamauchi, S. Ito, H. Miyasaka, H. Ishihara, and Y. Tsuboi, *J. Am. Chem. Soc.*, **2013**, *135*, 6643.
104. S. J. Yoon, J. Lee, S. Han, C.-K. Kim, C. W. Ahn, M.-K. Kim, and Y.-H. Lee, *Nat. Commun.*, **2018**, *9*, 2218.
105. A. Lenshof, C. Magnusson, and T. Laurell, *Lab Chip*, **2012**, *12*, 1210.
106. T. Laurell, F. Petersson, and A. Nilsson, *Chem. Soc. Rev.*, **2007**, *36*, 492.
107. M. Wu, A. Ozcelik, J. Rufo, Z. Wang, R. Fang, and T. J. Huang, *Microsyst. Nanoeng.*, **2019**, *5*, 32.
108. J. Shi, D. Ahmed, X. Mao, S. C. Lin, A. Lawit, and T. J. Huang, *Lab Chip*, **2009**, *9*, 2890.
109. X. Ding, S. C. Lin, B. Kiraly, H. Yue, S. Li, I. K. Chiang, J. Shi, S. J. Benkovic, and T. J. Huang, *Proc. Natl. Acad. Sci. U. S. A.*, **2012**, *109*, 11105.
110. L. Meng, F. Cai, P. Jiang, Z. Deng, F. Li, L. Niu, Y. Chen, J. Wu, and H. Zheng, *Appl. Phys. Lett.*, **2014**, *104*, 073701.
111. J.-L. Thomas, R. Marchiano, D. Baresch, *J. Quant. Spectrosc. Radiat. Transfer*, **2017**, *195*, 55.
112. D. Foresti and D. Poulikakos, *Phys. Rev. Lett.*, **2014**, *112*, 024301.
113. T. Kanazaki, S. Hirawa, M. Harada, and T. Okada, *Anal. Chem.*, **2010**, *82*, 4472.
114. A. Miyagawa, Y. Inoue, M. Harada, and T. Okada, *Anal. Sci.*, **2017**, *33*, 939.
115. A. Miyagawa, M. Harada, and T. Okada, *Anal. Chem.*, **2018**, *90*, 13729.
116. A. Miyagawa, M. Harada, and T. Okada, *ACS Sens.*, **2018**, *3*, 1870.
117. A. Miyagawa, M. Harada, and T. Okada, *Anal. Chem.*, **2018**, *90*, 2310.
118. A. Miyagawa, Y. Okada, and T. Okada, *ACS Omega*, **2020**, *5*, 3542.
119. T. Masudo and T. Okada, *Anal. Chem.*, **2001**, *73*, 3467.